Journal of The Electrochemical Society, **166** (6) C101-C107 (2019)
0013-4651/2019/166(6)/C101/7/$38.00 © The Electrochemical Society

Mechanistic Investigation on the Effect of Molybdate on the Critical Pitting Temperature of 2205 Duplex Stainless Steel

Razieh Tavassolian,[1,z] Mohammad Hadi Moayed,[1,z] and Iman Taji[1,2,z]

[1]*Department of Materials and Metallurgical Engineering, Faculty of Engineering, Ferdowsi University of Mashhad, Mashhad 91775-1111, Iran*
[2]*Department of Mechanical and Industrial Engineering, Norwegian University of Science and Technology, 7491 Trondheim, Norway*

In this research, a mechanistic approach was used to investigate the effect of molybdate ion on the critical pitting temperature (*CPT*) of 2205 duplex stainless steel. Firstly, the *CPT* of 2205 DSS was measured using potentiodynamic and potentiostatic polarization. It was found that with addition of 0.0005, 0.005 and 0.05 M Na_2MoO_4 to 0.5 M NaCl solution, the *CPT* increases approximately 4, 9, and 14°C, respectively. Using the lead-in pencil electrode technique, the mechanism by which molybdate ion influences the *CPT* was interpreted using the *CPT* model proposed by Salinas-Bravo and Newman. The results showed that molybdate has a negligible effect on the pit solution chemistry, resulting in a slight change in the diffusion-limited current density. However, it reduces the rate of alloy dissolution within the simulated pit solution, which was found as a reduced maximum current density.
© 2019 The Electrochemical Society. [DOI: 10.1149/2.1131904jes]

Manuscript submitted October 18, 2018; revised manuscript received February 28, 2019. Published March 14, 2019.

Duplex stainless steels (DSSs) are chromium-nickel-molybdenum-iron alloys which are usually characterized by the balance of the volume fraction of austenite and ferrite. DSSs are commonly used in many industries, such as petrochemical, chemical, offshore, nuclear, and pulp and paper due to their superior corrosion resistance and high mechanical strength.[1–3]

In spite of the high corrosion resistance of stainless steels, they suffer from different types of localized corrosion, mostly pitting corrosion. The passive film formed on stainless steel is not entirely intact and it contains some weak points, such as sulfide inclusions, precipitates, and other surface discontinuities. Some species known as aggressive anions can develop breakdown events on these weak points, resulting in the formation of an occluded region. Acceleration of the alloy dissolution in these occluded regions could result in deterioration of a small area which is known as pitting corrosion.[4–6]

Critical pitting temperature is defined as a transition threshold from metastable to stable pitting. Metastable pits never become stable below this temperature. So far, some models have been proposed with respect to the definition of *CPT*. Based on a model proposed by Salinas-Bravo and Newman,[7] the *CPT* is the temperature at which the maximum current density equals to the limiting current density at the bottom of a salt-covered pit (i.e. $i_{lim} = i_{max}$). Based on this model, at temperatures lower than the *CPT*, the current density is not high enough for salt film precipitation; consequently, the pit solution is not aggressive enough to prevent repassivation. However, at temperatures above the *CPT*, the salt film can precipitate on the pit's surface, which stabilizes pit growth. This model has been successfully used to study the mechanism by which various parameters such as inhibitors (nitrate,[8] dichromate,[9] thiosulfate),[10] surface roughness,[11] and solution annealing temperature[12] can affect the *CPT*. However, the model cannot predict the exact value of the *CPT* which is usually measured using flat electrodes. Nevertheless, this discrepancy does not refute the model. Laycock et al.[13] proposed another definition for the *CPT*: the temperature below which salt precipitation acts as an intermediary in oxide passivation, like iron in sulphuric acid, while above the *CPT*, salt causes pit stability. Based on the pit chemistry, the *CPT* was described by Ernst and Newman[14] as the temperature at which $C_{sat} = C^*$, where C_{sat} represents the cation saturation concentration essential for salt precipitation and C^* is the critical concentration to sustain stable pit growth. Recently, Li, Scully and Frankel have proposed a new model that considers two different current densities: the maximum pit dissolution current density at the pit surface ($i_{diss,max}$) and the critical diffusion current density associated with maintenance of the critical local environment ($i_{diff,crit}$). The criterion for pit stability is defined as the maximum pit dissolution current density to be equal to or greater than the diffusion current density associated with critical concentration at the pit surface ($i_{diss,max} \geq i_{diff,crit}$).[15] However, more empirical findings are required to support the latter model.

Sodium molybdate is a non-toxic corrosion inhibitor which is used for both steel and also non-ferrous alloys.[16–23] Many mechanisms have been proposed to explain how molybdate ion inhibits the corrosion process. The main mechanisms include (i) blocking the active sites such as inclusions,[24,25] (ii) local acidity reduction in the pit cavity[24,25] and (iii) deposit in the film oxide which restricts the anion diffusion by repulsion forces or improvement the protectiveness of oxide layer.[24–27] Ilevbare and Burstein[25] investigated the effect of molybdate inhibition on the pitting corrosion of 304 and 316 stainless steels. They showed that the number and the size of metastable pits in both alloys were reduced in the presence of molybdate ions. Using potentiodynamic polarization, Refaey et al.[24] showed that increasing the concentration of molybdate anion causes a marked shift of the pitting potential toward noble values. Deyab and Abd El-Rahim[28] similarly reported that the rate of pit initiation decreases and pitting potential shifts toward more positive potentials by the addition of molybdate in carbonate formation water containing Cl^- ion. Moreover, the composition of the passive film was assessed using energy dispersive X-ray spectroscopy (EDX) and X-ray photoelectron spectroscopy (XPS) and MoO_2 and MoO_3 on were detected in the passive film formed on carbon steel. Although the beneficial effect of molybdate ion on the *CPT* of 2205 DSS has been studied previously,[29] important questions about the role of molybdate in the pit chemistry remained unanswered. In the present research, the effect of molybdate ion on the *CPT* of 2205 DSS was investigated by utilizing the lead-in pencil electrode technique. The pit chemistry was evaluated in terms of i_{lim} and i_{max} in 0.5 M NaCl and 5 M HCl solution with and without molybdate ions. Possible role of molybdate on the *CPT* was evaluated using Salinas-Bravo and Newman's *CPT* model.

Experimental

Material and test setup.—A plate of 2205 duplex stainless steel with the chemical composition shown in Table I was used in this study. To eliminate heat-treatment history, the as received plates were solution annealed at 1050°C for 45 min, followed by water quenching. This heat-treatment procedure dissolves all secondary phases formed previously.[12,30] Two types of samples were fabricated as the working electrode. For the *CPT* measurements, samples with surface area of

Table I. Chemical composition of 2205 DSS (wt%).

Element	C	Ni	Mn	Si	Cr	Mo	V	N	W	Fe
Wt%	0.02	5.30	1.18	0.50	21.61	3.07	0.14	0.15	0.06	Bal.

[z]E-mail: tavasolian.razie@yahoo.com; mhmoayed@um.ac.ir; iman.taji@ntnu.no

4 cm^2 were used to ensure reproducibility of results.[31] In order to avoid crevice corrosion at the metal/mount interface, the samples were pre-passivated in 0.1 M Na_2SO_4 at the anodic potential of 850 mV (SCE) for 10 min.[32,33] Specimens were mounted in epoxy resin and were connected to a copper wire. Before immersion into the test solution, the samples were mechanically wet ground by silicon carbide (SiC) emery papers up to 1200 grit, washed with ethanol and distilled water, and dried with warm air flow.

To study the pit chemistry, the pencil electrode was used as a working electrode with dimensions of 200 μm × 200 μm. Similarly, each pencil electrode was mounted in epoxy resin and was connected to a shielded copper wire. Before each test, the samples were wet-ground with 60 grit SiC paper, rinsed with ethanol and distilled water, and dried under flowing warm air. The exposed surface area of each pencil electrode was accurately calculated using image processing software, MIP. The surface area was in the range of $3 \times 10^{-4} \sim 6 \times 10^{-4}$ cm^2. The pencil electrode was placed facing up in the test solution to avoid convection inside the pit.

The electrolyte was 0.5 M NaCl, containing sodium molybdate at different concentrations. All electrochemical tests were conducted in a conventional three electrodes cell. A platinum plate with 2 cm^2 surface area and saturated calomel electrode (SCE) were used as the counter electrode and the reference electrode, respectively. The electrochemical measurements were carried out at 20, 30, 40, 45, 50, 60 and 70°C using a water bath.

Electrochemical measurement.—To determine the *CPT* of 2205 DSS at various concentrations of molybdate ion, potentiodynamic and potentiostatic polarization experiments were used. Firstly, open circuit potential (*OCP*) was measured for 15 min. The specimens were then polarized potentiodynamically at a sweep rate of 1 $mV.s^{-1}$ from 50 mV below the *OCP* up to a potential where a sudden increase in the current density, about 300 $\mu A.cm^{-2}$, was observed due passivity breakdown. Each potentiodynamic polarization was repeated at least three times to ensure reproducibility. The breakdown potential (E_b) was measured at aforementioned temperatures and plotted vs. temperature. The *CPT* is determined as the temperature at which a sharp decrease in E_b from the transpassive region to the pitting corrosion region was observed.

Potentiostatic *CPT* measurements were performed at the anodic potential of 750 mV (SCE) whilst the temperature was increasing at a rate of 0.5°C.min^{-1} until the current density continuously exceeded more than 100 $\mu A.cm^{-2}$. *CPT* for potentiostatic polarization was considered as the temperature at which the current density reached 100 $\mu A.cm^{-2}$. To ensure reproducibility, each test was repeated at least five times.

To measure the limiting current density, polarization was conducted in two-step processes, consisting of potentiostatic polarization at 850 mV (SCE) for 4000 s followed by potentiodynamic polarization from 850 mV (SCE) to −300 mV (SCE) at a sweep rate of 1 $mV.s^{-1}$. The current density and potential vs. time obtained during the artificial pit polarization are illustrated in Fig. 1. During the polarization at the high anodic potential of 850 mV (SCE), several small pits formed on the pencil electrode, consequently, the current density increased abruptly, as shown in Figure 1. Then, these small pits coalescenced and formed a single pit, followed by precipitation of a salt film on the pit surface. After this sequence, reverse potentiodynamic polarization was performed until salt layer dissolves completely. The limiting current density was measured at the salt-free (point b in Fig. 1). Details of the experimental procedure can be found elsewhere.[8,12,14] The artificial pit experiments were repeated at least 10 times at 50, 60 and 70°C. In order to eliminate the effect of pit depth on i_{lim}, 1-D pits were grown to more than 600 μm (more than threefold of the specimen width). The pit depth (a) was calculated using Faraday's second law, measuring the total current passed during metal dissolution in the two-step test.

$$a = \frac{Z}{n\mathrm{F}\rho} \int idt \qquad [1]$$

where Z is the mean alloy atomic weight (55.2 $g.mol^{-1}$), ρ is the alloy density (7.87 $g.cm^{-3}$), n is the stoichiometric dissolution of main alloying element including, Fe, Cr and Ni (2.23), and F is the Faraday's constant.

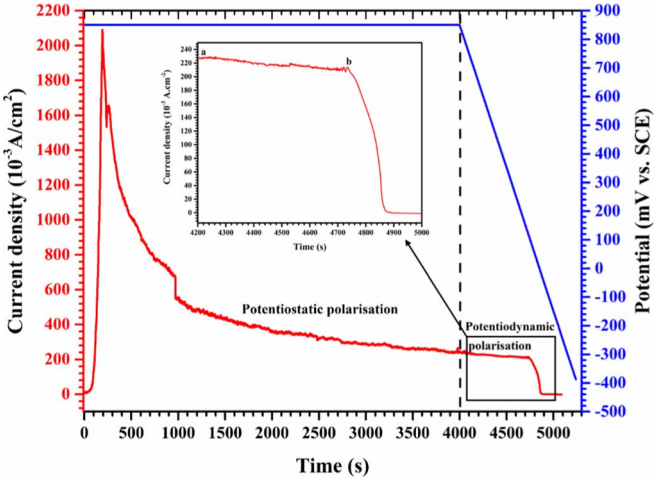

Figure 1. Current density vs. time curves obtained from two-step polarization: 1) potentiostatic polarization at 850 mV (SCE) for 4000 s and 2) potentiodynamic polarization from 850 mV (SCE) to cathodic potentials by 1 $mV.s^{-1}$ sweep rate.

The maximum current density was measured by polarizing the pencil electrode in in 5 M HCl and 5 M HCl + 0.05 M Na_2MoO_4 solutions, to simulate pit electrolyte at various temperatures.[7] Before starting the test, the *OCP* was recorded for 15 min. Then, potentiodynamic polarization was performed by sweeping the potential at a rate of 5 $mV.s^{-1}$ from −50 mV to 2500 mV with respect to the *OCP*. Each test was repeated three times to obtain reproducibility.

Results and Discussion

CPT measurements.—Figure 2 illustrates the anodic polarization curves obtained in 0.5 M NaCl containing various concentrations of molybdate ion. These curves were plotted on linear axes for a better demonstration of changes in breakdown potential. A decrease in the breakdown potential is observed as the temperature increases for all solutions. In Fig. 2a, an increase in the current density at the temperature range of 20–40°C is due to transpassive dissolution at the anodic potential of 950 mV (SCE). A sudden drop in E_b at 45°C suggests a transition from transpassivity to pitting corrosion. As can be seen from Fig. 2b, the breakdown potential increased to higher values in the presence of 0.0005 M sodium molybdate. Transpassivity occurred at the temperature range of 20–45°C while the transition from transpassivity to pitting corrosion takes place at around 50°C with the corresponding potential of 650 mV (SCE). A significant increase in E_b is observed by adding 0.005 M Na_2MoO_4 which shows no pitting corrosion up to 50°C. The beneficial effect of molybdate ion can be observed in 0.05 M molybdate ion which leads to a considerable increase in E_b. Current spikes below E_b in Fig. 2, are attributed to nucleation and repassivation of metastable pits.[34]

For better comparison, E_b is plotted as a function of temperature in Fig. 3. An increase in molybdate ion concentration causes a shift of the *CPT* to higher values. As shown in Fig. 3, the *CPT* of 2205 DSS in 0.5 M NaCl solution is a temperature between 40 and 45°C because E_b decreased noticeably at 45°C due to pitting corrosion. Previous studies reported the *CPT* of 2205 DSS in NaCl solution at a temperature range of 45–60°C.[12,29,31,35,36] Addition of 0.0005 M Na_2MoO_4 increases the range of *CPT* by about 5°C. It might be misinterpreted that the dramatic decline in E_b happened at 60°C, however, in this case, the *CPT* is considered at 50°C due to large error bar which indicates both pitting and transpassivity processes. Similarly, it is obvious that *CPT* is a temperature between 50 and 60°C in the presence of 0.005 M molybdate ion. It is slightly difficult to determine the *CPT*

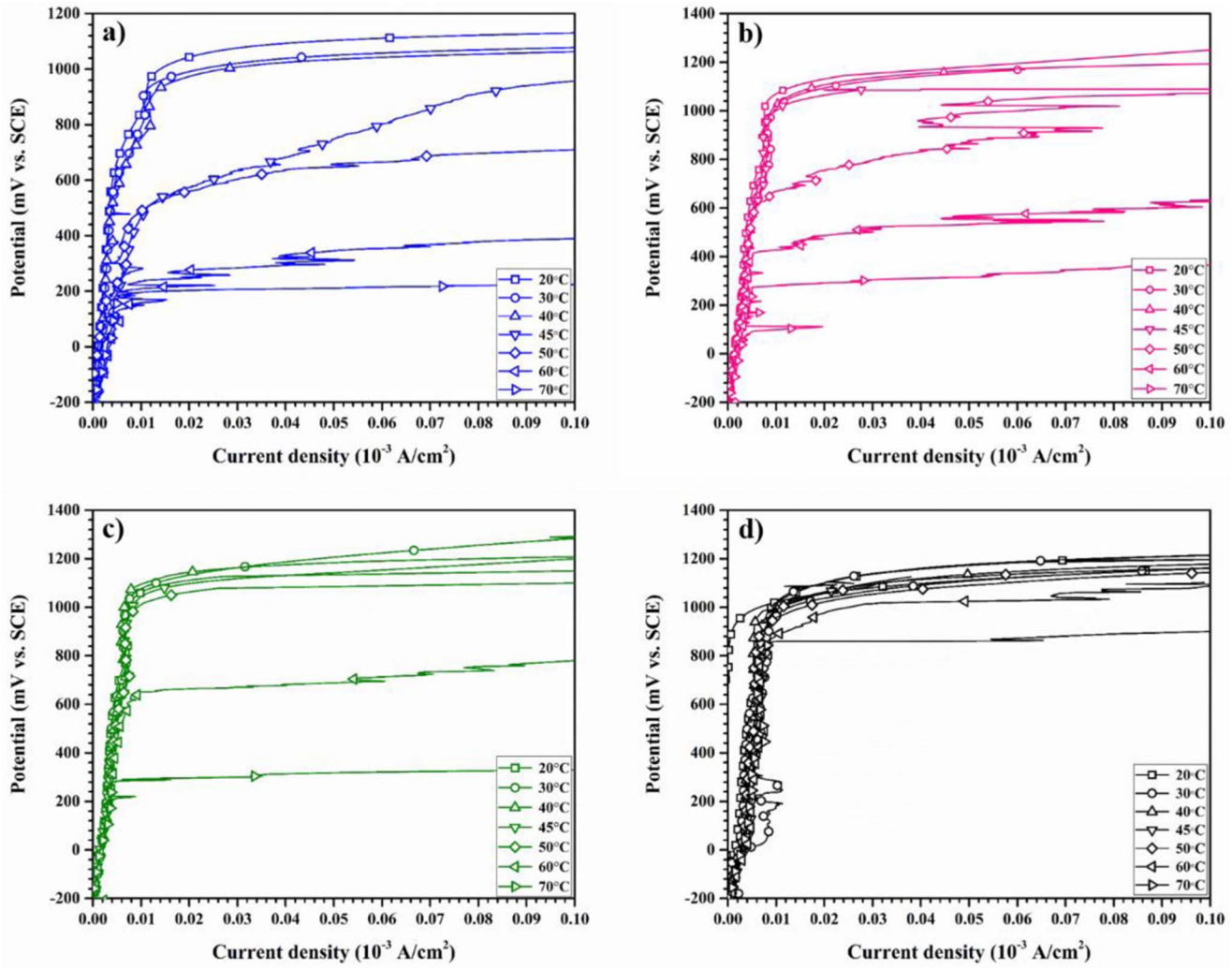

Figure 2. Potentiodynamic polarization curves of 2205 DSS at various temperatures in a) 0.5 M NaCl, b) 0.5 M NaCl + 0.0005 M Na_2MoO_4.

in the presence of 0.05 M Na_2MoO_4 because there is no marked drop in E_b up to 70°C. Therefore, it can be concluded that in the presence of 0.05 M molybdate ion, the *CPT* of 2205 DSS was high enough that the pitting potential reached the transpassive potential, therefore, it is difficult to determine the *CPT* value from this curve. After each potentiodynamic test, all of the samples were examined by optical microscope (OM) to confirm whether pitting happened. OM observations showed that pitting corrosion occurred at 60°C in the presence of 0.05 M Na_2MoO_4.

Figure 4 illustrates the results of *CPT* measurements at various molybdate ion concentrations employing potentiostatic polarization. It is obvious that addition of molybdate ions to chloride solution leads to an increase in the measured *CPT* value. Additionally, the *CPT* reaches higher values by increasing the molybdate concentrations. There are some current transients in the potentiostatic curves shown in Fig. 4, which are related to the nucleation and repassivation of metastable pits.[37]

The results of *CPT* measurements by potentiodynamic and potentiostatic techniques are shown in Fig. 5 vs. the ratio of molybdate to chloride concentrations. Each point for potentiostatic *CPT* measurement denotes the mean value and the error bar gives 90% confidence limit calculated from 5 separate runs. As shown in Fig. 5, the mean values of the *CPT* in the presence of 0.0005, 0.005 and 0.05 molybdate ions are around 56.5, 58 and 64°C, respectively. For the potentiodynamic *CPT* measurement, however, a range of *CPT* value is usually reported because the exact value of *CPT* is difficult to determine.[9,29,36] Therefore, to compare the *CPT* values obtained by the two techniques, the mean value relating to the transition range of transpassivity to pitting temperature is plotted in Fig. 5. It can be seen that the *CPT* values obtained by the potentiostatic method are higher than those obtained by potentiodynamic testing. Peguet et al.[31] reported that in potentiostatic tests most surface inclusions are dissolved before reaching the *CPT*, which lead to a decrease in pit nucleation sites. Furthermore, the passive film is reinforced in the potentiostatic polarization at temperatures below the *CPT*. Accordingly, a higher value of *CPT* is expected in the potentiostatic method compared to the potentiodynamic one.

Pencil electrode studies.—To have a better understanding about the mechanism of molybdate on increasing the *CPT*, the lead-in pencil electrode technique was employed and i_{lim} and i_{max} were determined in the presence of molybdate. A pencil electrode is a small diameter wire which is used to produce a single pit. Using this kind of electrode, one can investigate the different parameters of pit chemistry. For simplicity, the experiments were conducted only in two solutions with the composition of 0.5 M NaCl and 0.5 M NaCl + 0.05 M Na_2MoO_4.

Measuring the pit solution chemistry in the presence and absence of molybdate.—In order to measure the i_{lim}, two-step polarization which was described in the experimental section, was used and the limiting current densities and pit depths were obtained at temperatures of 50, 60 and 70°C. In Fig. 6, the results of $i_{lim}.a$ have been plotted against temperature so that the effect of molybdate ions on the

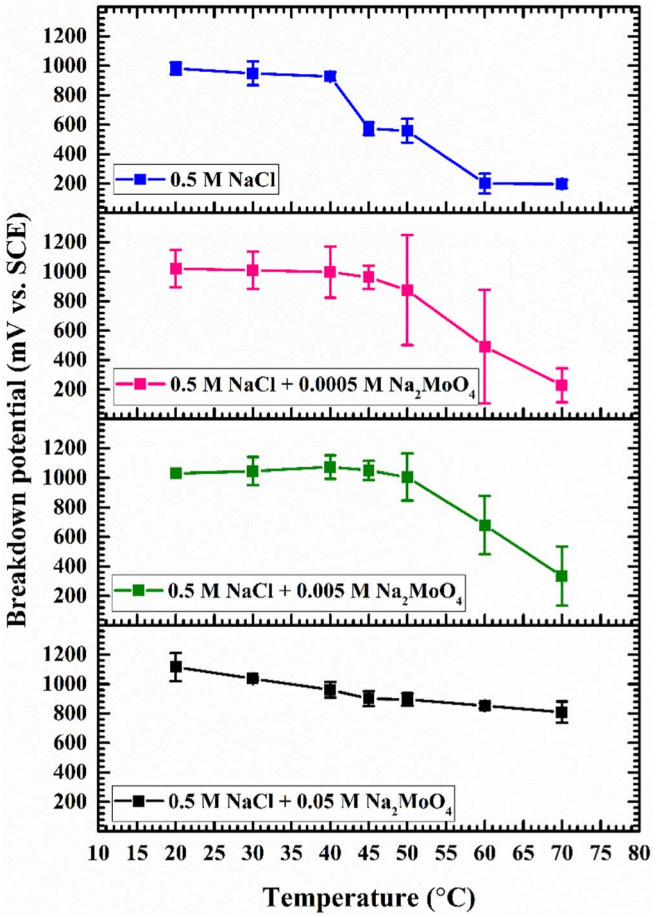

Figure 3. Mean value of breakdown potentials (E_b) as a function of the temperature at different molybdate concentrations obtained from potentiodynamic polarization. Error bars have been calculated with 90% confidence intervals.

pit solution chemistry can be compared more accurately. For two-step experiments, the product of $i_{lim}.a$ is a better demonstration rather than the i_{lim} because it takes into account the effect of pit depth. Each point in the graph denotes the mean value of 10 separate experiments with its corresponding error bar. In a 0.5 M NaCl containing solution, the mean value of $i_{lim}.a$ for temperatures of 50, 60 and 70°C were 12.8, 13.9 and 15.9 mA.cm^{-1}, respectively, whereas adding 0.05 M molybdate decreased $i_{lim}.a$ to the values of 12.2, 13.1 and 14.9 mA.cm^{-1}, respectively. It is obvious that $i_{lim}.a$ shifts toward higher values linearly with increasing temperature. In addition, the values of $i_{lim}.a$ in the presence of 0.05 M molybdate ions are marginally lower than those in 0.5 M NaCl solution. According to Eq. 2, the values of $i_{lim}.a$ are directly proportional to DC_{sat}. Therefore, it can be deduced that in the presence of molybdate the saturation concentration required for salt precipitation is lower.

$$i_{lim} = \frac{nF\,DC_{sat}}{a} \qquad [2]$$

Measuring the maximum current density in the presence and absence of molybdate.—The maximum current density can be obtained by potentiodynamic polarization of a pencil electrode in 5 M HCl solution. Based on Galvele's 1-D pit model,[4,6] when the active dissolution is dominant inside the occluded area of the pit, the pit solution becomes more acidic due to the hydrolysis of the metal cations. In order to maintain the charge electroneutrality in the pit anolyte, the chloride ions migrate into the pit solution. Therefore, it is expected that a solution with low pH and high concentration of chloride forms

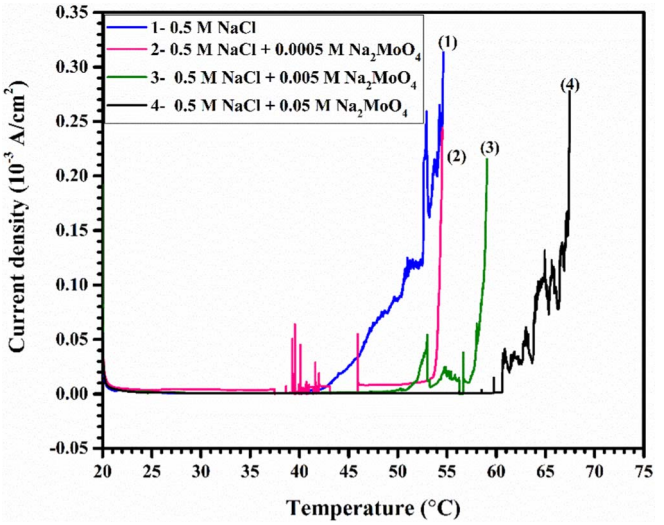

Figure 4. Current density-temperature curves obtained from potentiostatic polarization at the anodic potential of 750 mV (SCE). The temperature increased at a rate of 0.5°C.min^{-1}.

within an active pit. These extreme conditions provide conditions for pit growth with no repassivation. It is reported that 5 M HCl could be a good estimation to simulate the pit anolyte.[7,38] Consequently, testing in this solution provides an analogous condition for alloy dissolution in the pit cavity.

Fig. 7 illustrates the results of potentiodynamic polarization of a pencil electrode in 5 M HCl solution with and without molybdate ions. The tests were conducted at the temperatures of 20 to 70°C with an increment of 10°C. The potentiodynamic curve consists of a primary increase of current density and then a sudden decrease which is leveled off after a while. Such a decrease in current density can be originated from two reasons 1) the passivation of the alloy surface below the *CPT* as well as 2) formation of supersturated electrolyte at the pit surface leading to salt precipitation above the *CPT*. The current density caused by salt layer has featured with existing some fluctuations which might be attributed to local passivation and reactivation under the salt.[8,12] In addition, it is apparent from Fig. 7 that the current density associated

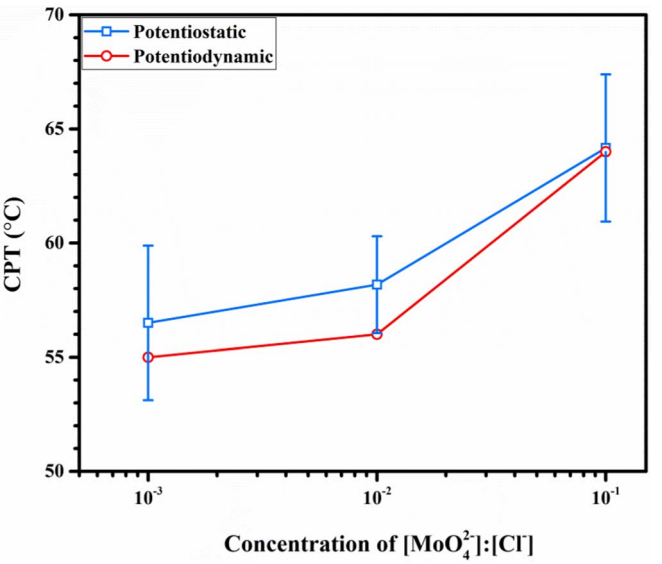

Figure 5. Mean value of *CPT* as a function of the molybdate to chloride ratio obtained from potentiodynamic and potentiostatic polarization. Error bars have been calculated with 90% confidence intervals in potentiostatic teste.

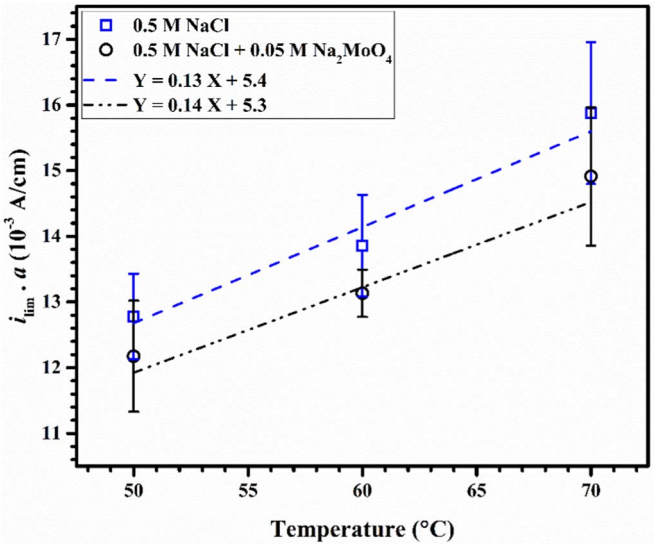

Figure 6. The product of limiting current density and pit depth versus temperature curves for 2205 DSS pencil electrode obtained from two-step polarization in 0.5 M NaCl and 0.5 M NaCl + 0.05 M Na_2MoO_4. Error bars have been calculated with 90% confidence intervals.

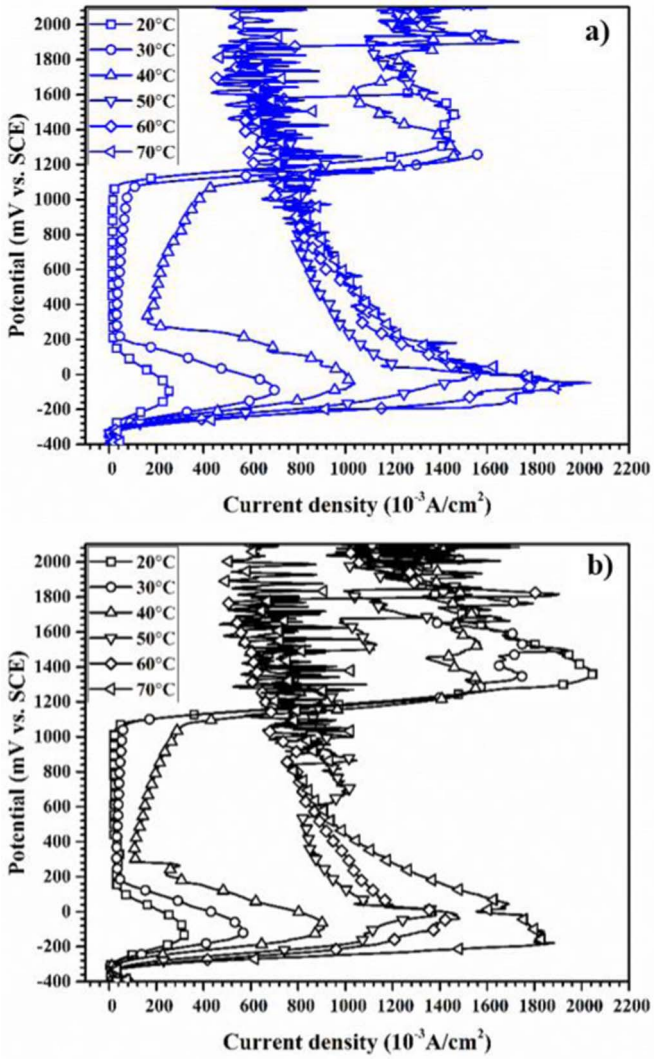

Figure 7. Potentiodynamic polarization curves of 2205 DSS pencil electrode in a) 5 M HCl and b) 5 M HCl + 0.05 M Na_2MoO_4 solutions.

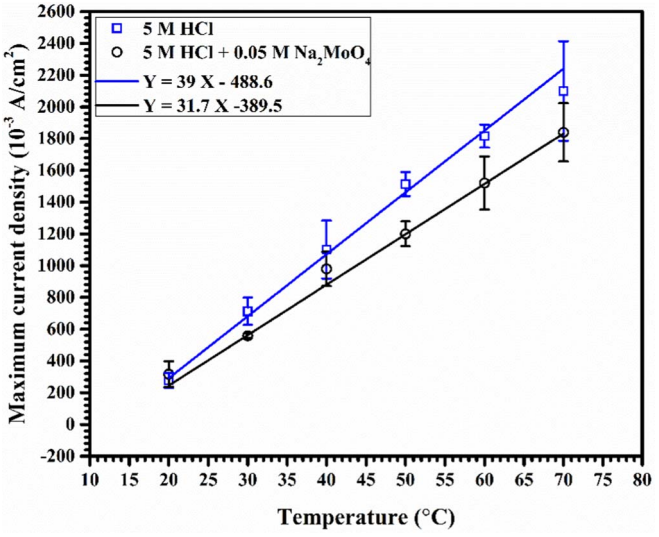

Figure 8. Mean value of the maximum current density of 2205 DSS pencil electrode as a function of the temperature obtained from potentiodynamic polarization in simulated pit solution with and without molybdate ion. Error bars have been calculated with 90% confidence intervals.

with diffusion control is much higher than its corresponding value when the metal is passivated. From Fig. 7 it can be inferred that in temperatures equal or lower than 40°C, after reaching the maximum current density, the metal passivated while it has actively dissolved above 50°C, and then it went under diffusion-controlled status for both solutions of 5 M HCl and 5 M HCl + 0.05 M Na_2MoO_4. Additionally, the breakdown observed at high anodic potentials at the temperature range of 20 to 40°C stems from the transpassive dissolution which confirms that the electrode surface was in the passivity region. However, the value of the current density at 40°C (about 200 $mA.cm^{-2}$) is considerably high relative to the values which are known as passive current densities. The reason of such high value could be explained by the fact that 40°C is the transition temperature from passivity to dissolution under the salt. At this temperature, the metal surface consists of regions where the alloy is passive as well as regions where dissolution of metal occurs. In other words, the overall measured current density is the sum of two currents: one associated to the dissolving part and the other to the remaining passive part. Optical observation of the alloy surface at an anodic potential of 600 mV (SCE) revealed preferential dissolution of austenite with no indication of ferrite dissolution at 40°C, whereas at the temperature of 60°C dissolution of both phases is observed. Thus, as discussed before, the *CPT* is most likely in the range of 40 to 50°C for both solutions. Furthermore, the i_{max} increases with temperature, as Fig. 7 shows. The mean values of i_{max} obtained from three independent potentiodynamic polarizations in different temperatures are shown in Fig. 8. As seen in Fig. 8, the i_{max} with the presence of molybdate in all temperatures is lower than that in molybdate free solution. However, the difference of i_{max} between these two solutions reduced as the temperature decreases and converged at about 20°C. The i_{max} for both solutions at 20°C is approximately 300 mA/cm^2 while at 70°C these values are 2100 and 1840 mA/cm^2 for 5 M HCl and 5 M HCl + 0.05 M Na_2MoO_4 solutions, respectively. It has been reported that other passivating inhibitors, like nitrate and dichromate, decrease the i_{max}.[8,9] Furthermore, it is reported that the variation of i_{max} as a function of temperature follows a linear trend.[8–10] Similarly, the i_{max} values shown in Fig. 8 increased linearly with increasing temperature.

Explanation of CPT increase in the presence of molybdate ion using Newman's model.—Potentiodynamic and potentiostatic polarization results showed that molybdate ion increases the *CPT* of 2205 DSS, which agrees with others.[29] To have a better understanding about the possible mechanism, it is necessary to evaluate the influence of

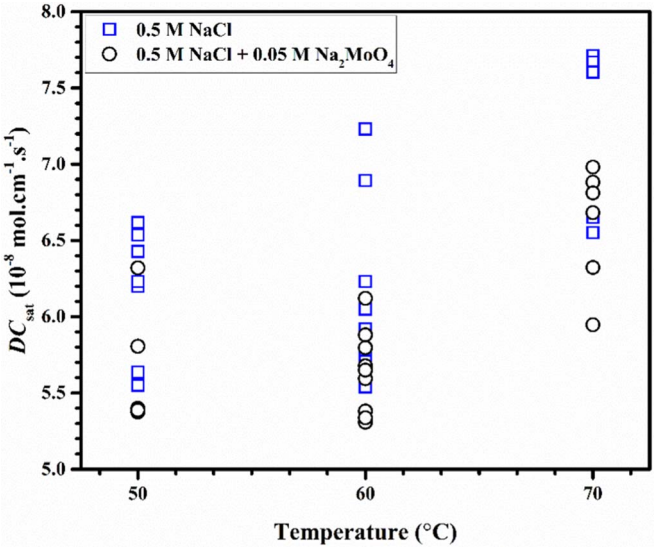

Figure 9. The DC_{sat} values of 2205 DSS pencil elctrode as a function of temperature in 0.5 M NaCl and 0.5 M NaCl + 0.05 M Na_2MoO_4.

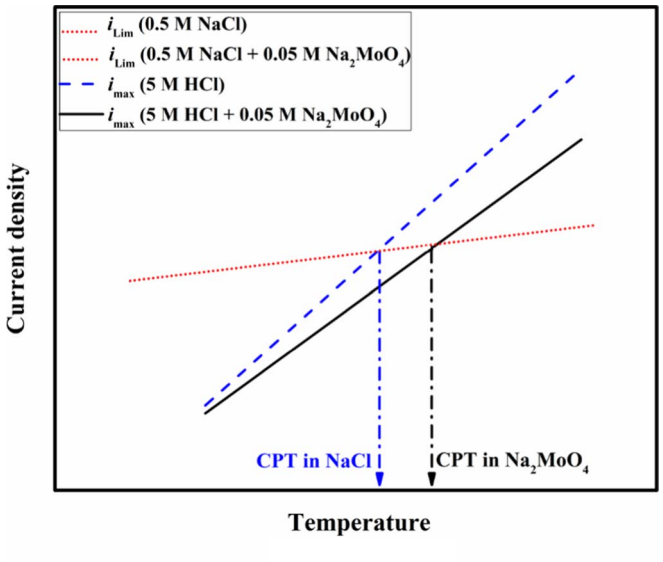

Figure 10. A schematic of i_{lim} and i_{max} vs. temperature curves that shows how molybdate ion can be affected the *CPT* of 2205 DSS based on Salinas-Bravo and Newman's model.

molybdate on the pit chemistry and the rate of alloy dissolution by measuring i_{lim} and i_{max} in simulated pit solution. Salinas-Bravo and Newman[7] proposed that the critical pitting temperature is the temperature at which $i_{max} \geq i_{lim}$. Therefore, *CPT* could be affected in two ways:

1) A change of the saturation concentration of metal cations (C_{sat}), and consequently altering i_{lim} (Eq. 2).
   This mostly happens in the presence of inhibitive or aggressive anions in bulk solution when they diffuse into the pit cavity. They might be able to change the pit solution chemistry. A decrease in C_{sat} means that lower temperature is needed for salt precipitation while an increase in the C_{sat} implies that higher temperature is required for salt precipitation.[7] Zakeri and Moayed[8] reported that nitrate ion increases the *CPT* by increasing the value of DC_{sat} (i.e. the saturation concentration required for salt precipitation). It is also showed that thiosulphate is able to decrease the *CPT* by decreasing the DC_{sat} (facilitating salt precipitation).[10] Fig. 9 shows DC_{sat} values as a function of temperature in the presence and absence of molybdate. It is evident that molybate anion slightly decreased the value of DC_{sat}. The measured values of DC_{sat} in this research are comparable with previous results which have been reported in the range of $3 \times 10^{-8} \sim 9 \times 10^{-8}$ mol.cm^{-1}.s^{-1}[8,10,12,39]
2) A change in i_{max}. In order to stabilize a pit, dissolution rate in the pit cavity must be high enough to precipitate the salt. As shown, molydbdate has decreased the i_{max} in all measured temperatures and its influence on decreasing i_{max} is more evident at higher temperatures.

Based on the presented results, it is discerned that molybdate increases the *CPT* by decreasing i_{max} rather than changing the i_{lim}. To have a better comparison, i_{max} and i_{lim} are represented schematically in Fig. 10 as a function of temperature. Only one line is sketched to represent i_{lim} for the two solutions, because molybdate has a negligible effect of i_{lim}. It should be borne in mind that as the geometry of an artificial pit is different from that of an actual pit, the exact value of *CPT* measured on the bulk specimen cannot be predicted by Newman's model.[7] Indeed, Newmans's model is just a conceptual model; considering the point at which i_{max} equals to i_{lim}, and it could just rationalize the mechanism by which species can alter the *CPT*.

As Fig. 10 suggests, i_{lim} slightly increases with temperature, while the i_{max} notably changes with temperature. This change in the i_{max} leads to a change of the intersection point of i_{max} and i_{lim}, therefore, an increase in the *CPT* value for the containing molybdate solution. As a result, molybdate increases the alloy *CPT* by lowering the rate of dissolution in the pit solution, hence higher temperatures are required to reach the necessary concentration of metal cations for salt precipitation.

Conclusions

In this study, the influence of molybdate ion on the *CPT* of 2205 duplex stainless steel was investigated. Potentiostatic studies showed that the *CPT* increases from 50°C in 0.5 M NaCl to 66°C in 0.5 M NaCl + 0.05M Na_2MoO_4. Using pencil electrode experiments, it was found that molybdate ion slightly decreased DC_{sat} and i_{lim}. Additionally, the results of potentiodynamic polarization of a pencil electrode in simulated pit solution (5 M HCl) showed that the maximum current density (i_{max}) decreased in 5 M HCl + 0.05 M Na_2MoO_4. Based on Newman's model, it can be concluded that the intersection point of i_{max} and i_{lim} in the presence of molybdate shifts to higher temperature due to decrease in i_{max}. Accordingly, the *CPT* of 2205 DSS increases to higher value.

Acknowledgments

The authors acknowledge the financial support from Ferdowsi University of Mashhad under grant No. 3/42722 and the provision of laboratory facilities. Additionally, the authors express their gratitude for Prof. Frankel and Davood Nakhaie who patiently reviewed the manuscript and gave constructive comments. The raw/processed data required to reproduce these findings cannot be shared at this time due to technical or time limitations.

ORCID

Mohammad Hadi Moayed https://orcid.org/0000-0002-4296-8496

References

1. H. Liou, Y. Pan, R. Hsieh, and W. Tsai, **10**, 231 (2001).
2. Z. Zhang, D. Han, Y. Jiang, C. Shi, and J. Li, *Nucl. Eng. Des.*, **243**, 56 (2012).
3. S. D. Armas and I. A. Moreuil, *Duplex Stainless Steels*, p. 437, John Wiley & Sons, (2009).
4. J. Galvele, *Corros. Sci.*, **21**, 551 (1981).
5. M. G. Alvarez and J. R. Galvele, *Shreir's Corrosion*, p. 772, Elsevier, (2010).
6. J. R. Galvele, *J. Electrochem. Soc.*, **123**, 464 (1976).

7. V. M. Salinas-Bravo and R. C. Newman, *Corros. Sci.*, **36**, 67 (1994).
8. M. Zakeri and M. H. Moayed, *Corros. Sci.*, **85**, 222 (2014).
9. M. Zakeri, D. Nakhaie, M. Naghizadeh, and M. H. Moayed, *Corros. Sci.*, **93**, 234 (2015).
10. M. Naghizadeh, D. Nakhaie, M. Zakeri, and M. H. Moayed, *J. Electrochem. Soc.*, **162**, C71 (2014).
11. M. H. Moayed, N. J. Laycock, and R. C. Newman, *Corros. Sci.*, **45**, 1203 (2003).
12. M. Naghizadeh and M. H. Moayed, *Corros. Sci.*, **94**, 179 (2015).
13. N. J. Laycock, *J. Electrochem. Soc.*, **145**, 2622 (1998).
14. P. Ernst and R. C. Newman, *Corros. Sci.*, **44**, 943 (2002).
15. T. Li, J. R. Scully, and G. S. Frankel, *J. Electrochem. Soc.*, **165**, 484 (2018).
16. X. Li, S. Deng, and H. Fu, *Corros. Sci.*, **53**, 2748 (2011).
17. V. Moutarlier, M. P. Gigandet, and J. Pagetti, *Appl. Surf. Sci.*, **206**, 237 (2003).
18. K. H. Na and S. Il Pyun, *J. Electroanal. Chem.*, **596**, 7 (2006).
19. Y. qi Wang, G. Kong, C. shan Che, and B. Zhang, *Constr. Build. Mater.*, **162**, 383 (2018).
20. M. S. Vukasovich and J. P. G. Farr, *Polyhedron*, **5**, 551 (1986).
21. E. A. Lizlovs, *Corrosion*, **32**, 263 (1976).
22. K. C. Emregül and A. A. Aksüt, *Corros. Sci.*, **45**, 2415 (2003).
23. S. Z. El Abedin, *J. Appl. Electrochem.*, **31**, 711 (2001).
24. S. A. M. Refaey, S. S. Abd El-Rehim, F. Taha, M. B. Saleh, and R. A. Ahmed, *Appl. Surf. Sci.*, **158**, 190 (2000).
25. G. O. Ilevbare and G. T. Burstein, *Corros. Sci.*, **45**, 1545 (2003).
26. J. P. G. Farr and M. Saremi, *Surf. Technol.*, **19**, 137 (1983).
27. M. A. Stranick, *Corrosion*, **40**, 296 (1984).
28. M. A. Deyab and S. S. Abd El-Rehim, *Electrochim. Acta*, **53**, 1754 (2007).
29. F. Eghbali, M. H. Moayed, A. Davoodi, and N. Ebrahimi, *Corros. Sci.*, **53**, 513 (2011).
30. K. Vijayalakshmi, V. Muthupandi, and R. Jayachitra, *Mater. Sci. Eng. A*, **529**, 447 (2011).
31. L. Peguet, A. Gaugain, C. Dussart, B. Malki, and B. Baroux, *Corros. Sci.*, **60**, 280 (2012).
32. J. Jun, K. Holguin, and G. S. Frankel, *Corrosion*, **70**, 146 (2014).
33. S. Pahlavan et al., *Corros. Sci.*, **112**, 233 (2016).
34. I. Taji, M. H. Moayed, and M. Mirjalili, *Corros. Sci.*, **92**, 301 (2015).
35. M. Hoseinpoor, M. Momeni, M. H. Moayed, and A. Davoodi, *Corros. Sci.*, **80**, 197 (2014).
36. N. Ebrahimi, M. H. Moayed, and A. Davoodi, *Corros. Sci.*, **53**, 1278 (2011).
37. P. C. Pistorius and G. T. Burstein, *Philos. Trans. R. Soc. A Math. Phys. Eng. Sci.*, **341**, 531 (1992).
38. R. C. Newman and T. Shahrabi, *Corros. Sci.*, **27**, 827 (1987).
39. T. Li, J. R. Scully, and G. S. Frankel, *J. Electrochem. Soc.*, **165**, 762 (2018).